Studying gas flows in the SUNBIRD starburst galaxies and LIRGs: Gas flows in NGC 6000

P. Janse van Rensburg[1, 2], **K. M. Mogotsi**[1, 3], **P. Väisänen**[1, 3], **and M. A. Bershady**[1, 2, 4]

[1]South African Astronomical Observatory, PO Box 9, Observatory, 7935 Cape Town, South Africa
[2]Astronomy Department, University of Cape Town, Private Bag X3, Rondebosch 7701, South Africa
[3]Southern African Large Telescope, PO Box 9, Observatory, 7935 Cape Town, South Africa
[4]University of Wisconsin, Department of Astronomy, 475 North Charter Street, Madison, WI 53706, USA

E-mail: petro@saao.ac.za

Abstract. Gas flows are an important aspect of galactic feedback and the regulation of star formation in galaxies. Nearby starburst galaxies and LIRGs provide an extreme environment where feedback and the changes due to it can be studied in great detail. The aim of this project is to search for traces of outflows and inflows in a sample of nearby starburst galaxies and LIRGs in the SUNBIRD survey, and to characterize them using observations of the stellar, and neutral and ionized gas kinematics. As a first step, the gas flows were studied using long-slit spectra from the Southern African Large Telescope. We present preliminary results from this data for one of the SUNBIRD galaxies NGC 6000. The neutral and ionized gas kinematics can be traced through the NaD absorption lines and Hα emission line, respectively. In this proceeding, we modelled the ionized gas with multiple components of Gaussian and Gauss-Hermite functions and compared best-fit models as an initial step to identify and characterize the gas flows in and around this galaxy. In NGC 6000, a double Gaussian and Gaussian-Hermite function modeled the Hα emission line better which indicates that there could be outflowing, inflowing or extraplanar gas.

1. Introduction

Galaxies display a bimodal distribution in colour: red, early type galaxies with a low star formation rate and blue, late-type galaxies with a high star formation rate [e.g., 1]. This bimodality originates because gas can either be enhanced on quenched depending on the inflow and outflow of gas in the galaxy as well as gas heating. The inflow and outflow of gas is described by the baryon cycle. Gas accreting onto the galaxy from the intergalactic medium makes it possible for more stars to form. Gas that is flowing out of the galaxy can either leave the galaxy completely if it has a velocity greater than the escape velocity of the galaxy, flow to the circumgalactic medium, or it can be recycled back into the galaxy. Galaxies with a high star formation rate create an extreme environment where the baryon cycle is easier to study and observe with earth-based observations [2; 3].

Galactic outflows or winds are one of the primary feedback mechanisms in galaxies. Outflows

are mainly driven by star formation or active galactic nuclei (AGN) activity and is important in the regulation of star formation. They are also multi-phase and can be studied with various tracers [2]. For example, in the optical regime, stellar absorption and outflowing neutral gas can be traced with the sodium doublet (NaD) absorption lines and ionized gas with the Hα emission line [e.g., 4; 5]. Outflow velocities can also range from tens to a few hundred km/s [e.g., 4; 6].

In this project, we study the gas flows in nearby starburst galaxies and LIRGs in the SUperNovae and starBurst in the InfraReD (SUNBIRD) survey [7]. The SUNBIRD survey has two science goals: to calculate the total SFR in the nearby universe by looking at dust-enshrouded core-collapse supernovae in star forming galaxies, and to perform an in-depth study of star formation in LIRGs.

2. Observational Methods and Data Analysis

2.1. Sample and Observations

The SUNBIRD survey contains more than 40 galaxies. For this project, we focused on a subsample of 24 galaxies based on the availability of lower (R $\sim$ 1000) and higher (R $\sim$ 3000) resolution long-slit spectra from previous studies [8; 6]. The lower resolution data can be used for stellar population and kinematics modelling, as well as using the emission lines for line diagnostics and characterisation of the interstellar medium. The line diagnostics can be used to characterise the outflowing gas and determine if the outflow is driven by star formation, AGN activity or both. The higher resolution data is useful for more complex multi-component fitting of the emission and absorption lines which traces the ionized and neutral gas, respectively. The sub-sample includes isolated galaxies, Seyferts, AGNs, and galaxies in group/cluster environments, all covering a wide range of interaction stages. Figure 1 shows the interaction stages of the sub-sample and the general properties of the galaxies in the sub-sample are shown in Table 1.

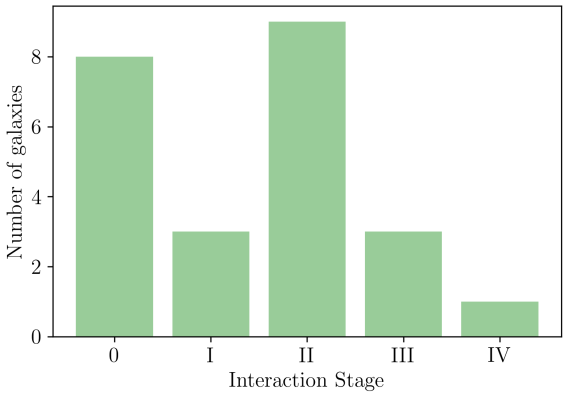

Figure 1: The interaction stages of the sub-sample ranging from isolated galaxies (0) to galaxies in a post-merger phase (IV).

The starburst galaxies and LIRGs in the SUNBIRD survey have been studied with long-slit spectra from the Southern African Large Telescope Robert Stobie Spectrograph [SALT, RSS; 9; 10] in two previous studies. In the study by [8], the author studied 52 SUNBIRD galaxies by looking at their stellar populations and the properties of the interstellar medium using spectra with a grating of PG0900 (R $\sim$ 1000), which covered a wavelength range of approximately 3640−6740 Å. In the study by [6], 40 SUNBIRD galaxies were studied using higher resolution (R $\sim$ 3000) spectra (PG1800 grating), covering a wavelength range of about 5600−6930 Å.

Table 1: Properties of the galaxies in the sub-sample.

Redshift	$0.0073 \leq z \leq 0.0482$ ($34 < D_L \leq 217$ Mpc)
IR luminosity	$10^{10.76} L_\odot \leq L_{IR} \leq 10^{11.81} L_\odot$
NIR SFR	$10^{0.99} \mathrm{M}_\odot \mathrm{yr}^{-1} \leq \mathrm{SFR} \leq 10^{2.04} \mathrm{M}_\odot \mathrm{yr}^{-1}$

The author studied outflows by looking at the kinematics of the ionized and neutral gas traced through the Hα emission line and NaD absorption lines, respectively. The kinematics were determined through fitting Gaussian and Gauss-Hermite models. If outflows were present in the galaxy, these were detected as deviations from regular galaxy rotation as well as differences between the Hα and NaD rotation curves. That work did not model the stellar contribution to the spectra. We aim to improve and extend the work done by [6] by performing more complex emission line fitting and modeling the stellar kinematics with a Penalized Pixel-Fitting method [pPXF, 11].

In order to get a better understanding of the properties of the sub-sample, we plotted the BPT [Baldwin, Phillips, and Terlevich; 12] diagram using the results from the two previous studies. This allowed us to differentiate the star-forming galaxies from the AGN in the sub-sample. This is shown in Figure 2a. In addition, we also plotted a Wide-field Infrared Survey Explorer [WISE; 13] colour-colour plot (W1-W2 vs W2-W3), shown in Figure 2b, to differentiate between the star-forming galaxies and LIRGs, and AGN. In Figure 2a, it shows that the majority of the galaxies in the sub-sample are either star-forming (HII) galaxies or they are in the composite region, where the power source can be star formation, an AGN or even shock excitation [14]. The WISE colour-colour plot shows a similar result with only two galaxies in the AGN/LINER/ULIRG region.

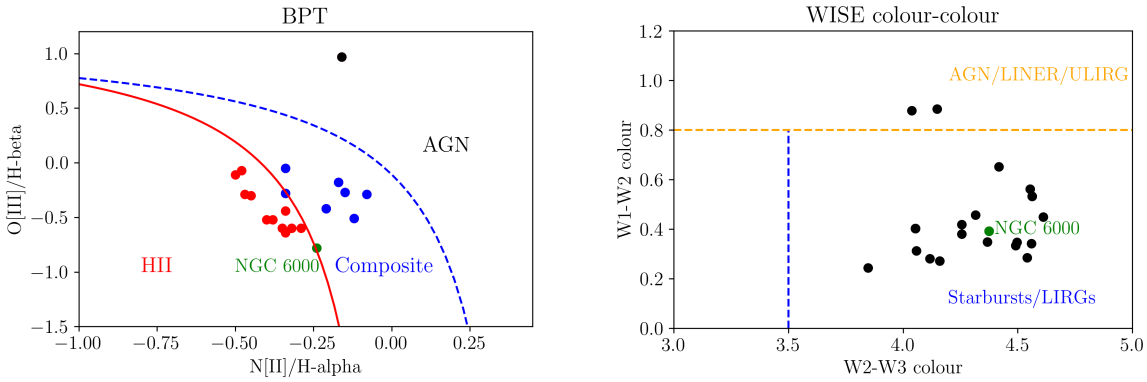

(a) BPT diagram of the sub-sample.

(b) WISE colour-colour plot of the sub-sample.

Figure 2: BPT diagram and WISE colour-colour plot of the sub-sample showing the differentiation between the star-forming galaxies and AGNs.

In this proceeding, we present preliminary results of one galaxy in the sub-sample: NGC 6000. All of the data were reduced using IRAF[1] by [8]. NGC 6000 is a nearby star-forming spiral galaxy at $z = 0.007$. It has an IR SFR of $10^{1.2}\mathrm{M}_{\odot}\mathrm{yr}^{-1}$ and an IR luminosity of $10^{10.97}L_{\odot}$. In the BPT diagram (Figure 2a), it is on the border between the HII and composite region and in the WISE colour-colour plot (Figure 2b) it is classified as a starburst/LIRG. Based on its IR luminosity, NGC 6000 would be classified as a starburst galaxy since LIRGs have an IR luminosity of $10^{11}L_{\odot} \leq L_{\mathrm{IR}} < 10^{12}L_{\odot}$ [15]. The rotation curve of this galaxy calculated by [6] is shown in Figure 3. The author also calculated an offset velocity between NaD and Hα of 140 km/s. In [6], only a single Gaussian and Gaussian-Hermite was fitted and the velocities were calculated with the overall best-fit model.

[1] Image Reduction and Analysis Facility, distributed by the National Optical Astronomy Observatory.

2.2. Emission line modeling

In order to build and improve on the work done by [6], three models were fitted to the SALT RSS long-slit spectra of the sub-sample to obtain the kinematics of the galaxies. Instead of selecting one model overall, we compare the three different models on a pixel by pixel basis. We first focused on obtaining the kinematics of the ionized gas, traced by the Hα emission line. Three emission lines were fitted: the two [NII] lines and the Hα line in the region between approximately 6550Å and 6700Å. Three models were fitted to the emission lines:

(i) A single Gaussian model on each emission line,

(ii) a single Gaussian model on the two [NII] emission lines and a double Gaussian model on the Hα emission line, and

(iii) a single Gaussian-Hermite model on each emission line.

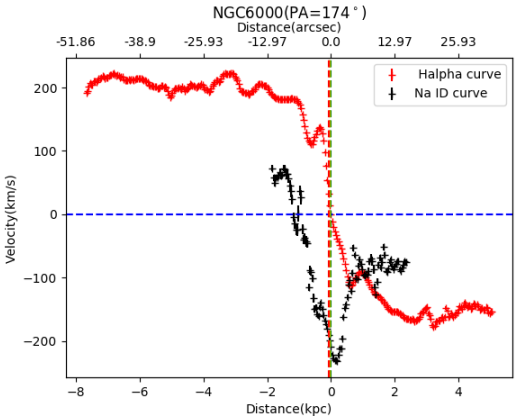

Figure 3: The rotation curve of NGC 6000 from [6]. The ionized gas traced by Hα is shown in red and the neutral gas traced by NaD is shown in black.

The Gaussian-Hermite has two additional parameters: skewness, which fits the wings and heaviness of the tails, and kurtosis, which fits the peak. The Gaussian-Hermite function becomes a normal Gaussian when these two parameters are 0.

An automated Python code was written to fit these three models to the emission lines and calculate the rotation curve of each galaxy based on the best fit at each pixel. The emission lines were fitted at each position (pixel) along the slit. Before the emission lines were fitted, the continuum around Hα and [NII] was modelled with a polynomial using the `specutils` Astropy package[2] and subtracted from the spectrum. The emission line modelling was performed through the non-linear least squares `kmpfit` package from the Kapteyn Python module[3]. We find that other Python-based software do not have the flexibility to easily adjust the models for the analysis we want to perform. An example of the double Gaussian model for two pixels is shown in Figure 5.

The initial parameters were determined based on the position (centroid) of the Hα line and known proximity of the two [NII] lines. We also added bounds to limit the standard deviation (width) of each emission line. Widths smaller than 0.422 Å would not be sensible because of the wavelength dispersion and widths larger than 20 Å would include regions outside the emission lines. We also applied a 4σ cut to exclude any pixels where the noise were modeled. A combined rotation curve was calculated by using the velocity from the best-fit model at each pixel, determined from the chi-squared value. A heliocentric velocity correction was also applied to the velocities.

3. Results

A preliminary rotation curve for NGC 6000 is shown in Figure 4. At each pixel, the velocity was determined by the model that fitted the best (smallest reduced chi-square value). The single

[2] https://specutils.readthedocs.io/en/stable/index.html
[3] https://www.astro.rug.nl/software/kapteyn/index.html

Gaussian model fitted the best at the edge of the galaxy. A double Gaussian function and Gaussian-Hermite (asymmetric profile) had the best fit in the rest of the galaxy. An example of a double Gaussian fit near the centre of the galaxy is shown in Figure 5a. The secondary component in the double Gaussian suggests that there could be inflows, outflows or extraplanar gas. The velocity offset between the broad and narrow component at the centre of the galaxy is about half of what was calculated in [6] (60 km/s), however it is still in agreement with other galaxy outflow velocities (see Section 1). In the work of [6], they only showed the rotation curve based on a single Gaussian component (refer to Figure 3), which only shows gas flows as deviations from regular galaxy rotation. By fitting an additional component, we can not only determine whether there are multiple gas components, but also study the properties of the gas flows.

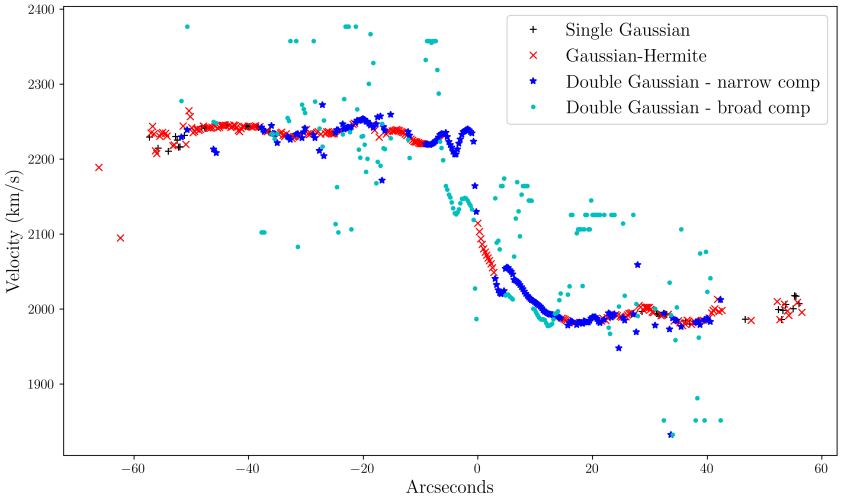

Figure 4: The rotation curve of NGC 6000. The velocity of the best fit is shown as black plus signs for a single Gaussian, red crosses for a Gaussian-Hermite function, and cyan dots and blue stars for the broad and narrow component of the Double Gaussian, respectively.

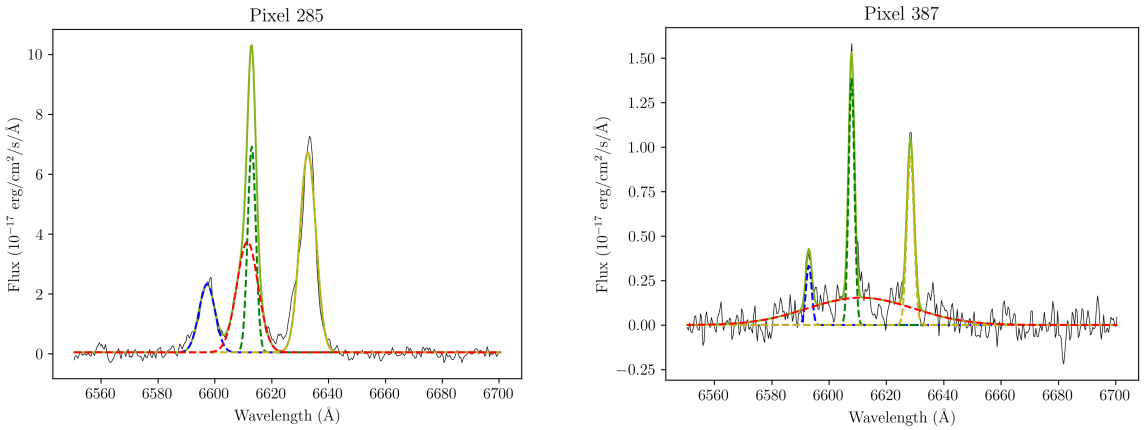

(a) Double Gaussian fit at pixel 285.

(b) Double Gaussian fit at pixel 387.

Figure 5: Double Gaussian fit of the Hα and [NII] emission lines near the centre of the galaxy (a) and in a region where the velocity is constant (b).

We note that there are some areas where better constraints are needed, especially in the broad component (cyan dots). There are also regions where the broad component velocity seems to remain constant (e.g., at 20 arcseconds). An example of a double Gaussian fit at this region is shown in Figure 5b. The narrow component velocity is not affected by the broad component, but the broad component has a velocity much greater than what we would expect in a secondary component. This suggests that it could be extraplanar gas or scattered light from the instrument. It will be investigated in further analysis.

4. Conclusion

We have shown preliminary results of a study of the gas flows in galaxy NGC 6000 based on long-slit spectra from the RSS on SALT. From the rotation curve, we showed that a double Gaussian and Gaussian-Hermite fit the spectrum better, especially near the centre of the galaxy. These assymetric functions indicate that there is some outflowing, inflowing or extraplanar gas. In the future, this analysis will be repeated for all other galaxies in the sub-sample and we will also study some of them with multi-wavelength data including data from the Atacama Large Millimeter/submillimeter Array (ALMA), the Multi Unit Spectroscopic Explorer [MUSE; 16] and the SALT NIR Integral Field Unit [IFU; 17]. In order to verify our analysis, we will also do a similar analysis with other software like Bayesian active galactic nucleus (AGN) Decomposition Analysis for Sloan Digital Sky Survey (SDSS) Spectra [BADASS; 18].

Acknowledgments

PJ acknowledges the support from the National Research Foundation of South Africa (NRF, Partial Postgraduate Scholarship UID: 142477) and the South African Astronomical Observatory (SAAO). The results presented in this proceedings are based on observations made with the Southern African Large Telescope (SALT) under the program 2013-1-RSA_OTH-024.

References

[1] Strateva I *et al.* 2001 *AJ* **122** 1861–74
[2] Veilleux S, Cecil G and Bland-Hawthorn J 2005 *ARA&A* **43** 769–826
[3] Tumlinson J, Peeples M S and Werk J K 2017 *ARA&A* **55** 389–432
[4] Cazzoli S, Arribas S, Maiolino R and Colina L 2016 *A&A* **590** A125
[5] Fluetsch A *et al.* 2021 *MNRAS* **505** 5753–83
[6] Tafere M S 2018 *UCT* Master's thesis
[7] Väisänen P *et al.* 2014 ed Y D Mayya D R G and Terlevich E (INAOE & AMC) pp 185–9
[8] Ramphul R A 2018 *UCT* Ph.D. thesis
[9] Burgh E B *et al.* 2003 ed Iye M and Moorwood A F M (SPIE) pp 1463–71
[10] Kobulnicky H A *et al.* 2003 ed Iye M and Moorwood A F M (SPIE) pp 1634–44
[11] Cappellari M and Emsellem E 2004 *PASP* **116** 138–147
[12] Baldwin J A, Phillips M M and Terlevich R 1981 *PASP* **93** 5–19
[13] Wright E L *et al.* 2010 *AJ* **140** 1868–1881
[14] Kewley L J, Nicholls D C and Sutherland R S 2019 *ARA&A* **57** 511–570
[15] Sanders D B and Mirabel I F 1996 *ARA&A* **34** 749–792
[16] Bacon R *et al.* 2010 vol 7735 ed McLean I S, Ramsay S K and Takami H (SPIE) pp 131–139
[17] Wolf M J *et al.* 2018 vol 10702 ed Evans C J, Simard L and Takami H (SPIE) pp 854–873
[18] Sexton R O, Matzko W, Darden N, Canalizo G and Gorjian V 2020 *MNRAS* **500** 2871–2895